

Flame balls for a free boundary combustion model with radiative transfer*

Jan Bouwe van den Berg¹, Vincent Guyonne^{1,2} and Josephus Hulshof¹

21st July 2005

¹ *Department of Mathematics, Vrije Universiteit Amsterdam, De Boelelaan 1081, 1081 HV Amsterdam, The Netherlands, email: janbouwe@few.vu.nl, vincent@few.vu.nl, jhulshof@few.vu.nl*

² *Université Bordeaux 1, Mathématiques Appliquées de Bordeaux, 33405 Talence cedex, France, email: vincent.guyonne@math.u-bordeaux1.fr*

Abstract

We study radial flame ball solutions of a three dimensional free boundary problem (FBP) which models combustion of a gaseous mixture with dust in a micro-gravity environment. The model combines diffusion of mass and temperature with reaction at the flame front, the reaction rate being temperature dependent. The radiative flux due to the presence of dust enters the equation for the temperature in the form of a divergence term. This flux is modeled by Eddington's radiative transfer equation. The main parameters are the dimensionless opacity and the ratio of radiative and thermal fluxes. We prove existence of spherical flame ball solutions for the FBP. Bifurcations diagrams are obtained, exhibiting the multiplicity of solutions. Singular limit cases of the parameter values are also discussed.

1 Introduction

Combustion processes in gaseous mixtures exhibit a variety of phenomena, such as propagating flame fronts, and, in zero- or microgravity situations, flame balls. The latter are perhaps harder to observe, but the advantage is that they are stationary. From a mathematical point of view they are easier to understand, namely as equilibria rather than traveling wave solutions of the mathematical models used to describe the combustion processes. From a physical point of view, because of the force and speed of the reaction, it is hard to do controlled experiments on flame fronts, whereas the combustion is much less violent in flame balls, which can be observed for prolonged periods of time at the costs of having to transfer the experiment to a microgravity environment. In any case, the high costs and experimental difficulties in combustion research highlight the need for a thorough understanding of the mathematical models.

*This work was supported by a CNRS/NWO grant and the RTN network Front-Singularities, HPRN-CT-2002-00274. JH is also supported by the CWI in Amsterdam, and JB by a NWO VENI grant.

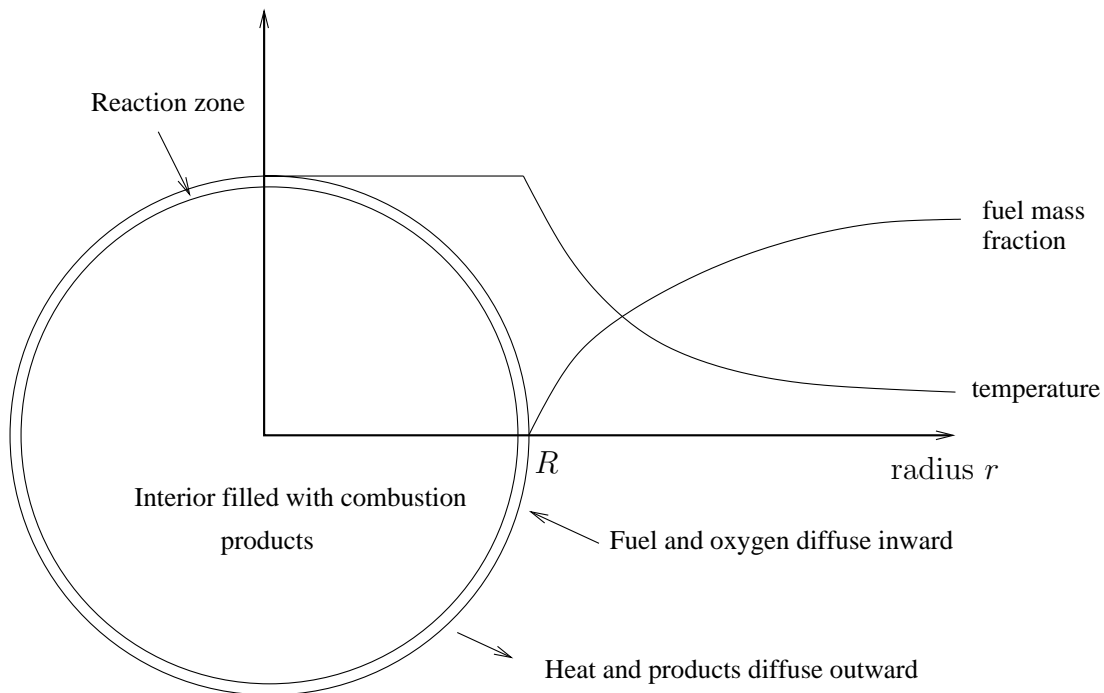


Figure 1: Profile of the temperature and the mass fraction variables in the adiabatic case. The radius of the flame ball is denoted by R , corresponding to the flame front.

Since the work of Zeldovich [1], flame balls are known to exist for models of combustion with simple chemistry, such as a one step reaction in which a gaseous reactant is converted into a gaseous product. Figure 1 is a sketch of a flame ball in the non-radiative case. Note that, in this particular situation, the burnt temperature θ_b is constant inside the ball. In this model, commonly referred to as the adiabatic case, flame balls are linearly unstable, in apparent agreement with the absence of experimentally observed flame balls. That was, until 1984, when Ronney discovered, by surprise, the existence, during drop tower experiments, of physical flame balls, later confirmed by experiments in the Space Shuttle. Since then, several effects have been taken into account in combustion models to explain stabilization of flame balls, in particular (radiative) heat losses from the combustion products inside the flame ball. We refer to [2] and references therein, see also the SOFBALL (Structure of Flame Balls at Low Lewis number) link on Paul Ronney's NASA home page [3].

In fact, the radiative transfer of heat in combustion processes taking place in inert, not fully transparent media (e.g. dust, porous media, ...), involves both emission and absorption of radiation, and may significantly influence the flame temperature (see Figure 2), its propagation speed, and the flammability of the medium itself. This occurs for instance in forest fires and fires in confined spaces, such as tunnels, and the importance of radiative transfer has been noted and stressed in [4, 5, 6]. In this paper, we concentrate on the effects of radiative transfer on flame balls.

There are two common formulations to model combustion processes: the reaction-diffusion and the free boundary formulation. Although both formulations are widely used in the combustion literature, the relation between the two approaches has so far largely been based on

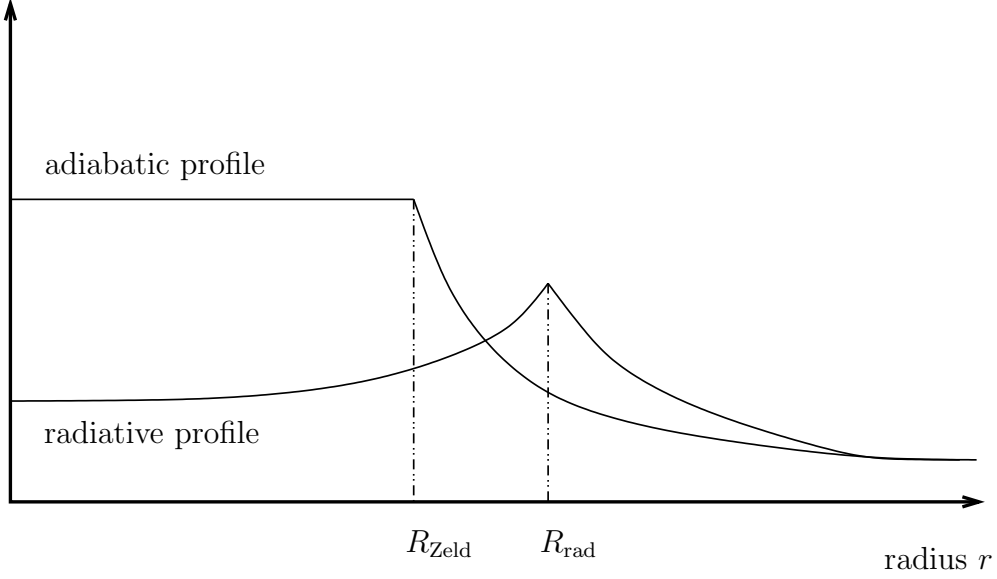


Figure 2: Difference of temperature profiles in the adiabatic and in the radiative case.

numerical simulation and heuristic arguments.

The basic thermo-diffusive model of combustion with simple chemistry is a Reaction Diffusion System (RDS) that is written as:

$$Y_t = \frac{1}{\text{Le}} \Delta Y - Y F(\theta), \quad (1a)$$

$$\theta_t = \Delta \theta + Y F(\theta), \quad (1b)$$

where Y denotes the mass fraction of the reactant, θ the temperature, and Le the Lewis number (ratio between conductivity and diffusivity). The function F is an Arrhenius type reaction rate involving a small parameter ε which is the inverse of the activation energy. The Arrhenius law is often modified by the choice of an ignition temperature, below which the reaction rate is taken to be zero. In this framework, (linearly) unstable flame balls are known to exist. For Lewis number close to unity, the growth of the radius has been described using an integro-differential equation which has been derived formally by Joulin [7] and rigorously validated by Roquejoffre et al. [8].

In the free boundary formulation the reaction is assumed to occur in a very thin region and the reaction diffusion system (1) is then approximated by a simpler Free Boundary Problem (FBP):

$$Y_t = \frac{1}{\text{Le}} \Delta Y \quad \text{for } x \notin R(t), \quad (2a)$$

$$\theta_t = \Delta \theta \quad \text{for } x \notin R(t), \quad (2b)$$

with

$$[\theta] = Y = 0, \quad -[\theta_n] = \frac{1}{\text{Le}} [Y_n] = F(\theta), \quad \text{for } x \in R(t), \quad (2c)$$

where $R(t)$ represent the location of the free boundary (the flame front), and brackets denote jumps across the free boundary (in the direction of the normal n). The mass flux into the

flame is balanced by (reaction) heat flux coming out of the flame, with a (predominantly) temperature dependent reaction rate. Note that at the flame front we impose the condition that $Y = 0$. Usually, one imposes only that the jump $[Y] = 0$, silently assuming that $Y \equiv 0$ on the burnt side of the flame front. Without such an assumption, the FBP formulation with $[Y] = 0$ instead of $Y = 0$ is underdetermined. As a free boundary problem this model should not be confused with the well-studied NEF model for nearly equidiffusional flames, which was derived by Sivashinsky by means of an asymptotic analysis, in which he coupled the deviation of the Lewis number from unity to ε , the inverse of the activation energy, see [9, 10], and derived what is now known as the Kuramoto-Sivashinsky equation.

The free boundary model (2) does not rely on any assumptions concerning the Lewis number. In its own right it is quite natural, even though its derivation from the RDS formulation has only been justified formally [11]. Its validity is also confirmed by numerical simulations on the RDS, and its great advantage is that several analytical aspects are simpler to treat.

The next step is to model the radiation effects. A microscopic description of the radiative transfer is given by the equation

$$\partial_t I + \Omega \cdot \nabla I = \sigma(B(\nu, \theta) - I),$$

where $I = I(x, t, \Omega, \nu)$ is a total radiative intensity, x the position, t the time, Ω the direction of emission vector, ν the frequency, σ the opacity of the medium and $B(\nu, \theta)$ the Planck distribution: $B(\nu, \theta) = \frac{2h\nu^3}{c^2}(\exp(\frac{h\nu}{k\theta}) - 1)^{-1}$. Since numerical simulations of this model are very cumbersome, radiation is most commonly described by simplified models, such as the (Milne-)Eddington diffusion equations, valid in the limit of isotropic radiation, the Rosseland model, valid for high opacity media, or the optically thin model, valid for nonabsorbent media ([12, 13]).

In this paper we adopt the Eddington diffusion model ([12, 13, 14, 15, 16, 17]), namely,

$$-\nabla(\nabla \cdot q) + 3\alpha^2 q = -\alpha \nabla \theta^4, \quad (3)$$

where q is the radiative flux. Thus, the radiative effects are a direct consequence of temperature variations. Following Joulin and Buckmaster [4, 5, 6], these radiative effects couple back to the temperature equation, in which the divergence of the radiative flux appears with coupling constant β , the Boltzmann constant. Thus β is a measure of the ratio between the radiative and the diffusive flux. For flame fronts, this extended model was proposed and studied in [4, 5, 6], and in [18, 19].

In this paper we study equilibria of the resulting FBP in the radially symmetric case, i.e. steady spherically symmetric flame balls. If we set $r = |x|$, we may thus write the Laplacian operator as $\Delta = \partial_{rr} + \frac{2}{r}\partial_r$, so that the problem can be viewed as a system of ordinary differential equations. Hence, throughout the paper all functions depend on the radial coordinate r only, and they all have zero derivative at $r = 0$. To make the mathematical analysis easier, we do not use the vector equation (3) but work with the scalar equation

$$-\Delta u + 3\alpha^2 u - \alpha \Delta \theta^4 = 0,$$

where $-u = \nabla \cdot q$, the divergence of the radiation flux as it appears in the modified temperature equation. The free boundary problem reads

$$\frac{1}{\text{Le}} \Delta Y = 0 \quad \text{for } r \neq R, \quad (4a)$$

$$-\Delta \theta - \beta u = 0 \quad \text{for } r \neq R, \quad (4b)$$

$$-\Delta u + 3\alpha^2 u - \alpha \Delta \theta^4 = 0. \quad (4c)$$

Equation (4c) is satisfied in the whole space in the sense of the distributions (and classically for $r \neq R$). The jump conditions at $r = R$ are

$$[\theta] = Y = 0, \quad -[\theta_r] = \frac{1}{\text{Le}}[Y_r] = F(\theta(R)), \quad (4d)$$

with u being continuous, while the size of the jump in u_r follows automatically from (4c) and (4d). The asymptotic boundary conditions are

$$Y \rightarrow Y_f, \quad \theta \rightarrow \theta_f, \quad u \rightarrow 0 \quad \text{as } r \rightarrow \infty. \quad (4e)$$

The parameters θ_f and Y_f denote the temperature and the mass fraction far away in the fresh region. We recall that R is the free boundary variable corresponding to the flame front and that $F(\theta(R))$ is the reaction rate evaluated at $r = R$. Note that we will not specify the reaction rate and work only with general reaction rates F . The reason is that, to prove existence properties, we only need to know that F is a positive function of the temperature at the flame front. The main result of this paper is the following:

Theorem 1 (Existence). *Let $\alpha \geq 0$, $\beta \geq 0$, let F be continuous and positive and let $\theta_f > 0$, $Y_f > 0$. Then there exists a radial solution $(\theta(r), Y(r), u(r), R)$ to (4). Moreover, for generic choices of the parameters the number of solutions is odd.*

Let us briefly outline the method of the proof. We first observe that the FBP formulation, with the Arrhenius law only acting on the flame front, allows to decouple equation (4a) for Y from the two others, (4b) and (4c). The only bounded function Y which solves (4a) and satisfies $Y = 0$ at $r = R$ and $Y \rightarrow Y_f$ as $r \rightarrow \infty$, is given by

$$Y(r) = \begin{cases} 0 & \text{for } r \leq R, \\ Y_f \left(1 - \frac{R}{r}\right) & \text{for } r > R. \end{cases} \quad (5)$$

Here R is still unknown. We now drop one of the free boundary condition, namely the last equality in (4d), and solve the problem with R as a parameter. In other words, we drop the reaction rate and fix R . The next theorem provides us with a unique solution of the resulting reduced problem, parameterized by the now prescribed flame ball radius R .

Theorem 2 (Uniqueness and existence for R fixed). *Fix $R > 0$ and let $\alpha \geq 0$, $\beta \geq 0$, $\theta_f > 0$, $Y_f > 0$. Then there exists a unique solution $(\theta_R(r), Y_R(r), u_R(r))$ to (4), with $\theta > 0$.*

To prove this theorem, we will first decompose the temperature as $\theta = \theta_h + w$ where θ_h is an adiabatic profile with an arbitrary fixed radius R . Because we seek radial solutions, we can explicitly compute θ_h , namely

$$\theta_h = \theta_f + \frac{Y_f}{\text{Le}} \min \left(1, \frac{R}{r} \right). \quad (6)$$

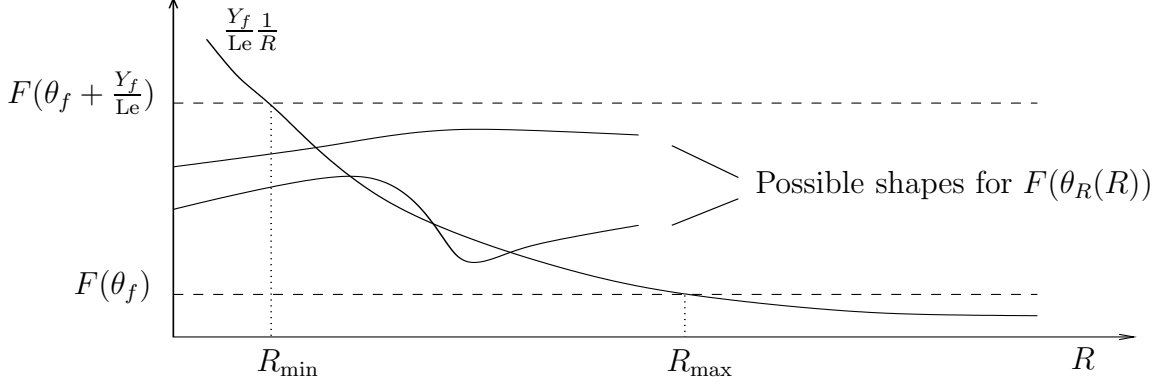


Figure 3: Sketch of the graphs occurring in Equation (7). The dashed lines are the bounds on $F(\theta_R(R))$; they are depicted here for the case of increasing F .

Then, we show that w satisfies a nonlinear elliptic equation defined on all \mathbb{R} . Thus θ_h is the temperature component of the solution of the reduced problem with given R , in the case that $\beta = 0$. The subscript h stands for “homogeneous”, because θ_h is the solution of the homogeneous part of (4b) which satisfies the jump condition. The other part w in the splitting will then be the solution of the full inhomogeneous equation (4b) which is smooth (i.e. $[w] = [w_r] = 0$) across $r = R$. Hence w satisfies the equation $-\Delta w = u$ globally, just as u solves (4c) globally, in the sense of the distributions. To solve this equation, we consider the problem on a bounded domain, more precisely on a ball $B_\rho = B(0, \rho) \subset \mathbb{R}^3$, with $\rho > R$ large. Using sub- and supersolution arguments, one obtains a solution on the bounded domain. Then we let $\rho \rightarrow \infty$, and, by a diagonal process, this leads to a solution on \mathbb{R}^3 . Uniqueness is proved using classical arguments (see Section 2 for details).

Remark 1. We only consider positive θ , the solution $\theta_R(r)$ depends continuously on R , and θ_R is bounded between θ_f and $\theta_f + \frac{Y_f}{Le}$.

Going back to the proof of Theorem 1, we need to find a value of R for which $\theta_R(r)$ satisfies the final free boundary condition in (4d). As we know Y explicitly, we are left with one “algebraic” equation

$$\frac{Y_f}{Le} \frac{1}{R} = F(\theta_R(R)). \quad (7)$$

Thus only at this final stage the reaction rate F plays a role in the analysis. From Figure 3 we can easily see that Equation (7) has at least one solution (see Section 2 for more details). This ends the proof of Theorem 1.

Remark 2. When solving Equation (7), one can easily see from Remark 1 and Figure 3 that the radiative radius R_{rad} is bounded between two values. If the reaction rate F is an increasing function of the temperature, as it is usually the case, the lower bound on the flame radius is given by the adiabatic or Zeldovich radius $R_{\text{Zeld}} = \frac{Y_f}{Le} \frac{1}{F(\theta_f + Y_f/Le)}$ (i.e. the radius in absence of radiative effects, see Section 2 for more details), whereas the upper bound is $\frac{Y_f}{Le} \frac{1}{F(\theta_f)}$.

In Section 3 we examine limit cases of Problem (4). The cases $\alpha \rightarrow \infty$ with β fixed, and $\alpha \rightarrow 0$ (or transparent limit) lead to the adiabatic case and are the easiest to justify.

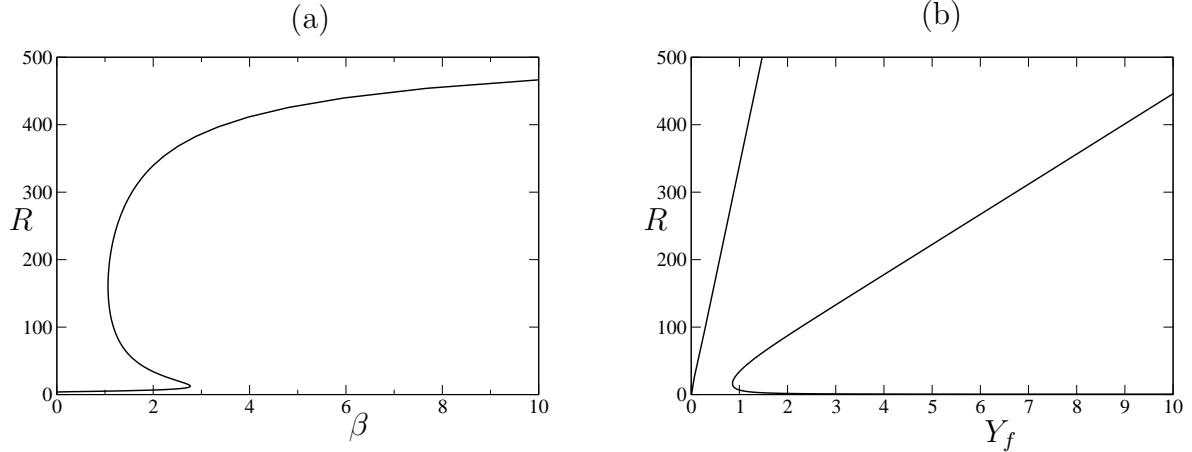


Figure 4: Bifurcation curves exhibiting turning points: (a) with β used as bifurcation parameter; (b) with Y_f as the parameter.

A more subtle analysis is needed to treat the cases $\beta \rightarrow \infty$ (large Boltzmann limit) and $\alpha \rightarrow 0$ supposing $\alpha\beta = \chi$ fixed (transparent limit combined with large Boltzmann numbers). In the large Boltzmann limit, we prove that the temperature profile converge to a constant profile, namely to the fresh temperature θ_f . On the other hand, in the transparent limit combined with large Boltzmann numbers, the temperature profile does not converge to a constant profile, but to a radiative one (cf. Figure 2).

Finally, in Section 4 we compare the analytic expressions in the asymptotic limits to numerical computations for the full problem. We also make a comparison with analytic calculations for a “linearized” system, see Section 4.1 for details. As an example, in Figure 4a we depict a typical bifurcation diagram, where β is used as the bifurcation parameter. For a range of parameter values there are three distinct flame ball solutions (for the adiabatic (non-radiative) problem there is always only one solution). Examining the corresponding solution profiles, the upper branch turns out to be physically irrelevant, since the temperature profile is almost identically equal to θ_f . In Figure 4b the fuel mass fraction Y_f in the fresh region is used as a bifurcation parameter. Again, multiple solutions are obtained, on two disconnected branches.

2 Existence of solutions

In this section we prove Theorem 2. We recall that in order to fix R , we consider Problem (4) and we drop the equation involving the reaction rate F in (4d). The expression for Y is of course given by (5). Theorem 1 follows immediately from Theorem 2 when we combine it with the fact that the algebraic equation (7) has a solution.

To begin with, we reduce equations (4b) and (4c) to one elliptic equation. To do so, we first need to introduce a splitting of the solution θ we are looking for, writing

$$\theta = \theta_h^R + w. \quad (8)$$

Here θ_h^R is the solution of

$$-\Delta\theta_h^R = 0 \quad \text{for } r \neq R, \quad (9a)$$

with jumps conditions

$$[\theta_h^R] = 0, \quad -\left[\frac{\partial\theta_h^R}{\partial r}\right] = \frac{1}{\text{Le}}\left[\frac{\partial Y}{\partial r}\right], \quad \text{at } r = R, \quad (9b)$$

and the asymptotic boundary condition

$$\theta_h^R \rightarrow \theta_f \quad \text{as } r \rightarrow \infty. \quad (9c)$$

We note that (9) can be solved explicitly, where θ_h^R is given by (6). The advantage of the splitting (8) is that w must have zero jumps:

$$[w] = [w_r] = 0,$$

and $w \rightarrow 0$ as $r \rightarrow \infty$. Hence it must be a solution of

$$-\Delta w = \beta u \quad (10)$$

on the *whole space* in the sense of the distributions.

Next we observe that (4c) implies that

$$u = \alpha(3\alpha^2 - \Delta)^{-1}\Delta\theta^4,$$

which expresses u in terms of θ^4 by means of the bounded operator

$$\alpha(3\alpha^2 - \Delta)^{-1}\Delta = \alpha\Delta(3\alpha^2 - \Delta)^{-1},$$

which operates from $L^\infty \rightarrow L^\infty$. Note that the Laplacian and its resolvent commute because $3\alpha^2 > 0$. Combining with (10), it follows that

$$\Delta(w + \alpha\beta(3\alpha^2 - \Delta)^{-1}\theta^4) = 0,$$

whence, since both w and θ^4 are bounded, $w + \alpha\beta(3\alpha^2 - \Delta)^{-1}\theta^4$ must be a constant:

$$w + \alpha\beta(3\alpha^2 - \Delta)^{-1}\theta^4 = C.$$

Subtracting θ_f^4 from θ^4 only changes the constant. Moreover, $\theta^4 - \theta_f^4$ has zero limit at infinity ($r \rightarrow \infty$), a property which is preserved by the resolvent $(3\alpha^2 - \Delta)^{-1}$, and also $w \rightarrow 0$ as $r \rightarrow \infty$. Thus $w + \alpha\beta(3\alpha^2 - \Delta)^{-1}(\theta^4 - \theta_f^4) = 0$. Applying $(3\alpha^2 - \Delta)^{-1}$ to both sides, we arrive at

$$(3\alpha^2 - \Delta)w + \alpha\beta((w + \theta_h^R)^4 - \theta_f^4) = 0, \quad (11a)$$

which again should hold globally, with asymptotic boundary condition

$$w \rightarrow 0 \quad \text{as } r \rightarrow \infty. \quad (11b)$$

We note that $w(r)$ is a solution of a second order ordinary differential equation (globally). Thus it has zero jumps $[w]$ and $[w_r]$ at $r = R$. We have split the problem for θ , which was

inhomogeneous because of the jump in $r = R$ and the nonzero limit as $r \rightarrow \infty$ on the one hand, and the presence of βu in (4b) on the other, into two parts. The first part, θ_h^R , takes care of the jumps and limits, while the second, w , corresponds to the inhomogeneous term βu in (4b).

Problem (11) for w will now be solved by first making a reduction to a bounded domain. The latter will be analyzed using monotonicity methods. A limit argument then gives the solution on the whole space. Uniqueness (and regularity) are also established.

2.1 Existence on a bounded domain

Let us consider (11) on a ball $B_\rho = B(0, \rho) \subset \mathbb{R}^3$, the boundary condition (11b) being replaced by $w = 0$ on ∂B_ρ . We assume $\rho > R$.

Lemma 3. *For fixed $0 < R < \rho$, there is a unique solution w of (11a) with $\theta = \theta_h^R + w \geq 0$ on B_ρ and $w = 0$ on ∂B_ρ . The solution is radial and as such it belongs to $C^2([0, \rho])$ as well as to $C^2(\overline{B_\rho})$. It satisfies the bounds*

$$-\frac{Y_f}{\text{Le}} \min\left(1, \frac{R}{|x|}\right) \leq w \leq 0. \quad (12)$$

Remark 3. *The estimate (12) is independent of the parameters α and β . It provides us with a uniform estimate on the decay rate of w towards zero as $r \rightarrow \infty$.*

Proof. We first establish the existence of w . The function $\overline{w} \equiv 0$ is a supersolution of (11a) with zero Dirichlet boundary data, because substituting $w = \overline{w} \equiv 0$ in (11a), we end up with $\alpha\beta((\theta_h^R)^4 - \theta_f^4) > 0$. On the other hand, the function $\underline{w} = -\frac{Y_f}{\text{Le}} \min(1, \frac{R}{r})$ is a subsolution: it is negative in $r = \rho$, and substituting $w = \underline{w}$ we obtain $3\alpha^2\underline{w} - \Delta\underline{w}$. The first term is negative, the latter too, but in the sense of the distributions. More precisely, $-\Delta\underline{w}$ is a negative “Dirac” measure supported on $r = R$. It is straightforward to mollify \underline{w} into a family of smooth subsolutions $\underline{w}^\varepsilon$ with $\underline{w}^\varepsilon \rightarrow \underline{w}$ uniformly as $\varepsilon \rightarrow 0$, and $\underline{w}^\varepsilon \equiv \underline{w}$ outside the interval $(R - \varepsilon, R + \varepsilon)$. By standard arguments, e.g. [20], it follows that there is a solution of (11a) with $w = 0$ in $r = \rho$ which lies between \underline{w} and \overline{w} . This solution is obtained using an iteration argument starting from either the sub- or the supersolution, both of which are radial. As a consequence, the constructed solution is also radial. The regularity of w , i.e. $w \in C^2(B_\rho)$, follows directly from ODE arguments. In fact the bounded solutions w of (11a) with $w = 0$ on ∂B_ρ are in $C^2(\overline{B_\rho})$, see again [20].

If w_1 and w_2 are two such solutions, then we set

$$f(x, w) = \alpha\beta((w + \theta_h^R(x))^4 - \theta_f^4),$$

and

$$c(x) = \int_0^1 \frac{\partial f}{\partial w}(x, tw_1(x) + (1-t)w_2(x)) dt.$$

The function $v = w_1 - w_2$ is a solution of

$$\begin{cases} -\Delta v + (3\alpha^2 + c(x))v = 0 & \text{in } B_\rho, \\ v = 0 & \text{on } \partial B_\rho, \end{cases}$$

where $c \in C(\overline{B_\rho})$. By the maximum principle, see [20], $v \equiv 0$ if c is nonnegative. Thus we have uniqueness in the class of functions w which satisfy $w(x) + \theta_h^R(x) \geq 0$, i.e., the functions w for which the corresponding temperature profile θ is positive, and it is natural to restrict to this class. This completes the proof. \square

Remark 4. Writing (11a) as an ODE, i.e.,

$$w'' = -\frac{2}{r}w' + 3\alpha^2 w + \alpha\beta \left((w + \theta_h^R(r))^4 - \theta_f^4 \right),$$

with initial conditions $w(0) = w_0$ and $w'(0) = 0$, this initial value problem is well-posed and behaves nicely in terms of continuous dependence on parameters. In particular, w , w' , w'' and w''' are uniformly bounded on bounded intervals (for bounded ranges of α^2 and $\alpha\beta$). Alternatively, to examine regularity, one could proceed from the PDE (11a) directly using bootstrap arguments and Hölder estimates for elliptic equations, see e.g. [20].

Remark 5. We emphasize that w is defined for $0 \leq r \leq \rho$ and that ρ as well as R are parameters with $0 < R < \rho$. Thus we write $w = w_\rho^R$.

2.2 Solutions on the whole space

In this section we take the limit $\rho \rightarrow \infty$ to prove existence of a solution w of Problem (11).

Lemma 4. For R fixed, there exists a solution w of Problem (11) which satisfies the bound (12). The solution belongs to $C^2(\mathbb{R})$ and is unique in the class of radial and non-radial functions.

Proof. Take a sequence $\rho_n \rightarrow \infty$ as $n \rightarrow \infty$, and set $w_n = w_{\rho_n}^R$, so w_n is a solution of

$$\begin{cases} -\Delta w_n + 3\alpha^2 w_n = -\alpha\beta \left((w_n + \theta_h^R)^4 - \theta_f^4 \right) & \text{in } B_{\rho_n}, \\ w_n = 0 & \text{on } \partial B_{\rho_n}, \end{cases}$$

as constructed in Section 2.1. We extend w_n to the whole of \mathbb{R}^3 by setting $w_n \equiv 0$ for $r \geq \rho_n$. Clearly estimate (12) continues to hold for w_n .

Now fix some $\rho = \bar{\rho}$ and consider the solutions w_n with $\rho_n > \bar{\rho}$, and in particular their restrictions to $B_{\bar{\rho}}$. It follows directly from Remark 4 that w_n and its first and second order derivatives are bounded and equicontinuous. Note that the nonlinear term in (11) is Lipschitz continuous if w is. Thus, we may extract a subsequence along which w_n converges in $C^2(\overline{B_{\bar{\rho}}})$. Choosing $\bar{\rho} = 1, 2, 3, \dots$ a standard diagonal argument now produces a subsequence along which w_n converges in $C^2(\overline{B_{\bar{\rho}}})$ for every $\bar{\rho} > 0$. It follows that the limit w exists on the whole space, and that it satisfies (11a) as well as the bound (12). Clearly w corresponds to a temperature profile $\theta = \theta_h^R + w > 0$ on \mathbb{R}^3 .

Now suppose we have two such profiles. Reasoning as in the uniqueness proof in Lemma 3 we find that $v = w_1 - w_2$ is bounded and satisfies

$$-\Delta v + (3\alpha^2 + c(x))v = 0 \quad \text{in } \mathbb{R}^3.$$

When $v \rightarrow 0$ as $|x| \rightarrow \infty$ (uniformly) the maximum principle implies that $v \equiv 0$, provided the coefficient $3\alpha^2 + c(x)$ of v is nonnegative. Thus we have uniqueness in the class of solutions w which have $w(x) \rightarrow 0$ as $|x| \rightarrow \infty$ uniformly. \square

2.3 Proof of Theorem 1

In the previous section we proved Theorem 2 and showed that, omitting the reaction rate from the problem formulation, there exists for every $R > 0$ a unique solution triple (θ, Y, u) with $\theta > 0$. It remains to solve (7) with $\theta_R(R)$ given by Theorem 2.

Remark 6. *In view of the estimate (12) the flame temperature $\theta(R)$ is bounded between θ_f and $\theta_f + \frac{Y_f}{Le}$. As F is a continuous positive function, let us define the positive numbers*

$$m = \min_{\theta \in [\theta_f, \theta_f + Y_f/Le]} F(\theta) \quad \text{and} \quad M = \max_{\theta \in [\theta_f, \theta_f + Y_f/Le]} F(\theta).$$

Then any solution of the full flame ball problem must satisfy

$$\frac{Y_f}{Le} \frac{1}{M} \leq R \leq \frac{Y_f}{Le} \frac{1}{m}. \quad (13)$$

Equation (7) has a left hand side which goes from $+\infty$ to 0 as R goes from 0 to ∞ . Its right hand side is bounded between m and M . Thus the existence of the solution in Theorem 1 is immediate once we know that Remark 1 (about continuity of $\theta_R(R)$) is true. More precisely:

Lemma 5. *If $R_n \rightarrow R > 0$, then the corresponding functions θ_{R_n} converge uniformly to θ_R on $[0, \infty)$.*

Proof. Clearly this will follow from the same statement for w_R , where w_R is the solution of (11) obtained in Lemma 4. In view of the bound (12), uniform convergence on bounded subsets implies uniform convergence on $[0, \infty)$. By exactly the same arguments as in the proof of Lemma 4 in Section 2.2, it follows that along a subsequence of $n \rightarrow \infty$, w_{R_n} (as well as its first and second order derivatives) converges uniformly on any bounded interval to a solution of (11) satisfying (12). Since this solution is unique, it follows that $w_{R_n} \rightarrow w_R$, along this subsequence. In fact, every sequence of $n \rightarrow \infty$ has a subsequence for which this is the case. But then there cannot be a sequence of n for which $\|w_{R_n} - w_R\|_\infty$ is bounded away from zero. This completes the proof of Lemma 5 and thereby of Theorem 1. \square

Remark 7. *Instead of using this sequence argument, one could also invoke an implicit function argument to conclude that $R \rightarrow \theta_R(R)$ (or $R \rightarrow w_R(R)$) is smooth. Furthermore, assuming the derivatives of left and right hand sides of (7) to be different at solutions, it follows immediately that the number of solutions is odd. This is the statement that in general situations the number of solutions is odd.*

2.4 Uniform estimates

As we have seen, solutions of the flame ball problem are given by $\theta = \theta_h^R + w_R$, where R is such that (7) holds, and where w_R is a C^2 -function (of course θ_h^R is not). Moreover, w_R satisfies (11). In this section we show that w is monotone in r , and that w belongs to $H^2(0, \infty)$.

Lemma 6. *The solution $w = w_R$ of (11) has $w' \geq 0$.*

Proof. w solves

$$-w'' - \frac{2}{r}w' = g(r, w) = -3\alpha^2 w - \alpha\beta \left((w + \theta_h^R(r))^4 - \theta_f^4 \right), \quad (14)$$

where g satisfies

$$\frac{\partial g}{\partial w} < 0 \quad \text{and} \quad \frac{\partial g}{\partial r} \geq 0,$$

the latter being discontinuous in $r = R$ of course, but with limits existing from both sides. Moreover, $w'(0) = 0$ by symmetry.

If w' is negative somewhere, then there must be points r_1 and r_2 such that $w'(r_1) = w'(r_2) = 0$, while $w' < 0$ on (r_1, r_2) . This follows from $w'(0) = 0$ and $0 > w(r) \rightarrow 0$ as $r \rightarrow \infty$.

Clearly then $g(r_1, w_1(r_1)) = -w''(r_1) \geq 0$ and $g(r_2, w_1(r_2)) = -w''(r_2) \leq 0$, contradicting

$$\frac{d}{dr}g(r, w(r)) = \frac{\partial g}{\partial r} + \frac{\partial g}{\partial w} \frac{\partial w}{\partial r} > 0 \quad \text{on } (r_1, r_2).$$

□

Lemma 7. *There exists a constant C depending on α^2 and $\alpha\beta$ such that*

$$\int_0^\infty w'(r)^2 dr < C.$$

Proof. Multiplying (14) by w and integrating from r_1 to r_2 ($0 < r_1 < r_2 < \infty$) we obtain

$$-\int_{r_1}^{r_2} w'' w dr = \int_{r_1}^{r_2} \frac{2}{r} w' w dr + \int_{r_1}^{r_2} g(r, w) w dr,$$

so that

$$\int_{r_1}^{r_2} |w'|^2 dr + w'(r_1)w(r_1) = w'(r_2)w(r_2) + \int_{r_1}^{r_2} \frac{2}{r} w' w dr + \int_{r_1}^{r_2} g(r, w) w dr.$$

Letting $r_1 \rightarrow 0$ and using $w' \geq 0$, $w < 0$, it follows that, also using (12),

$$\int_0^{r_2} |w'|^2 dr \leq \int_0^{r_2} g(r, w(r)) w(r) dr \leq C,$$

where C is a constant depending linearly on α^2 and $\alpha\beta$, but not on r_2 . This proves the claim. □

Going one step further, we get the following.

Lemma 8. *w belongs to $H^2(0, \infty)$.*

Proof. Multiplying (14) by $-w''$ and integrating from r_1 to r_2 we find

$$\int_{r_1}^{r_2} |w''|^2 dr + \int_{r_1}^{r_2} \frac{2}{r} w' w'' dr + \int_{r_1}^{r_2} g(r, w) w'' dr = 0.$$

Hence, with e.g. $r_1 = 2$,

$$\int_2^{r_2} |w''|^2 dr \leq \left(\int_2^{r_2} |w'|^2 dr \right)^{\frac{1}{2}} \left(\int_2^{r_2} |w''|^2 dr \right)^{\frac{1}{2}} + \left(\int_2^{r_2} |g(r, w(r))|^2 dr \right)^{\frac{1}{2}} \left(\int_2^{r_2} |w''|^2 dr \right)^{\frac{1}{2}}.$$

In view of (12), (14) and Lemma 7 we conclude that

$$\int_2^\infty |w''|^2 dr \leq C,$$

where C depends on α^2 and $\alpha\beta$. The fact that w is C^2 implies that also $\int_0^\infty |w''|^2$ is bounded. Lemma 7 and inequality (12) finish the proof. \square

Remark 8. *If we consider the problem in \mathbb{R}^3 , one can easily check that w belongs to $W^{2,p}(\mathbb{R}^3)$ if $p > 3$.*

3 Limit cases of the radiative parameters

In this section we examine some singular limit cases. We recall that we introduced the splitting $\theta = \theta_h^R + w$. Throughout this section, we consider a couple $(\theta_{\text{par}}, R_{\text{par}})$ depending on some parameters, and we seek a limit. Let us start by the following:

Remark 9. *As R_{par} lies in a compact set, see Remark 6, one can extract a subsequence converging to a limit, called R . Along the subsequence, $\theta_h^{R_{\text{par}}}$ converges to θ_h^R (uniformly).*

3.1 The limit case $\alpha \rightarrow \infty$ with β fixed

The limit $\alpha \rightarrow \infty$, β fixed is usually called the optically thick limit for an opaque medium. In this limit the effect of the radiation is lost. Indeed, we have

Lemma 9. *The solution w of Problem (11) converges to zero uniformly as $\alpha/\beta \rightarrow \infty$.*

As a consequence of this lemma, and in view of (13), the flame ball solution has a temperature profile that converges to the Zeldovich solution, and also the flame ball radius converges to the Zeldovich radius as $\alpha/\beta \rightarrow \infty$.

Proof. We simply modify the subsolution in the proof of Lemma 3 in such a way that it pushes the solution obtained in Lemma 3 and thereby w itself, to zero. A negative constant w is a subsolution provided

$$3\alpha^2 w + \beta\alpha ((\theta_h^R + w)^4 - \theta_f^4) \leq 0.$$

this is certainly the case if

$$\left(\theta_f + \frac{Y_f}{\text{Le}} + w\right)^4 - \theta_f^4 = -\frac{3\alpha}{\beta} w,$$

which has a unique solution $w \in (-\frac{Y_f}{\text{Le}}, 0)$, which is easily seen to converge to zero as $\alpha/\beta \rightarrow \infty$. This completes the proof. \square

Remark 10. *Note that the limit is the same as the one for α fixed and $\beta \rightarrow 0$, i.e. radiative flux negligible with respect to convective flux.*

3.2 The transparent limit $\alpha \rightarrow 0$ with β fixed

Surprisingly, as opposed to the traveling wave case, see [18], this limit also reproduces the adiabatic (Zeldovich) flames. As in the previous section we have

Lemma 10. *The solution w of Problem (11) converges to zero uniformly if $\alpha \rightarrow 0$ with β fixed.*

Proof. We have, in view of (12),

$$-\Delta w = -3\alpha^2 w - \alpha\beta((\theta_h^R + w)^4 - \theta_f^4) \rightarrow 0$$

uniformly, as $\alpha \rightarrow 0$ and $\alpha\beta \rightarrow 0$. Also, again because of (12), w is uniformly small for large r . By the maximum principle for the Laplacian this implies that $w \rightarrow 0$ uniformly as $\alpha \rightarrow 0$ and $\alpha\beta \rightarrow 0$. \square

3.3 Large Boltzmann numbers $\beta \rightarrow \infty$ with α fixed

With large Boltzmann numbers the solution loses its physical meaning because the temperature profile becomes flat. We have

Lemma 11. *For α fixed and $\beta \rightarrow \infty$ the temperature profile θ converges to θ_f uniformly.*

Proof. Let us set $w_n = w_{\beta_n}$, with $\beta_n \rightarrow \infty$ as $n \rightarrow \infty$. We are looking for a limit of the problem

$$-\Delta w_n = -3\alpha^2 w_n - \alpha\beta_n((\theta_h^{R_n} + w_n)^4 - \theta_f^4). \quad (15)$$

with asymptotic boundary condition $w_n \rightarrow 0$ as $|x| \rightarrow \infty$.

Writing the weak formulation of (15) and dividing by β_n we find that, for any test function $\varphi \in C_c^\infty([0, \infty))$, in view of (12),

$$\int ((\theta_h^{R_n} + w_n)^4 - \theta_f^4) \varphi = -\frac{1}{\beta_n} \int 3\alpha^2 w_n \varphi + \frac{1}{\alpha\beta_n} \int w_n \Delta \varphi \rightarrow 0 \quad \text{as } n \rightarrow \infty.$$

By the bound (12), the functions

$$(\theta_h^{R_n} + w_n)^4 - \theta_f^4 \quad (16)$$

are nonnegative. Thus we may conclude that they converge to the zero function in L_{loc}^1 strongly. Next, we rewrite (16) as

$$G(Z_{R_n} + w_n),$$

where $G(\xi) = (\theta_f + \xi)^4 - \theta_f^4$ and $Z_R(r) = \frac{Y_f}{\text{Le}} \min(1, \frac{R}{r})$.

Again in view of (12), the variable $\xi = Z_R + w$ ranges between 0 and Z_R . In this range G' is positive and bounded away from zero and infinity. Consequently, the functions $Z_{R_n} + w_n$ also converge strongly to zero in L_{loc}^1 . But Z_{R_n} converges if we restrict to a further subsequence, along which R_n converges, not only in L_{loc}^1 but also in L^∞ .

We claim that for any sequence R_n bounded away from zero and infinity, and for any sequence $\beta_n \rightarrow \infty$, the corresponding solutions w_n of (11) have the property that $\theta_n = \theta_h^{R_n} + w_n \rightarrow \theta_f$, uniformly on $[0, \infty)$. To prove this, we apply the following simple lemma.

Lemma 12. *Let f_n and g_n be functions on \mathbb{R}_+ such that*

- $f_n + g_n \geq 0$,
- $f_n + g_n \rightarrow 0$ in $L^1(0, \rho)$ for all $\rho > 0$,
- $f'_n \geq -C$ in a weak sense,
- $g'_n \geq 0$,

then $f_n + g_n \rightarrow 0$ in $L^\infty(0, \rho)$ for all $\rho > 0$.

Proof. Immediate from the estimate

$$f_n(r) + g_n(r) \geq f_n(r_0) + g_n(r_0) - C(r - r_0),$$

if $r > r_0 > 0$. □

This lemma applies to $f_n = Z_{R_n}$ and $g_n = w_n$, which is monotone by Lemma 6. As before, we conclude that $\theta_n - \theta_f \rightarrow 0$ in $L^\infty(\mathbb{R})$. □

3.4 The transparent limit combined with large Boltzmann numbers: $\alpha \rightarrow 0$ with $\alpha\beta = \chi$ fixed

Finally, we consider the limit $\alpha \rightarrow 0$, $\alpha\beta = \chi > 0$ fixed, which was also treated in the traveling wave context, see [18, 19]. We show that in this limit solutions of the radiative transfer problem converge to solutions of a radiative heat loss problem, where θ solves

$$\Delta\theta - \chi(\theta^4 - \theta_f^4) = 0 \quad r \neq R,$$

and R is the flame radius of the limit solution. This will follow along the same lines in the previous sections from

Lemma 13. *In the limit $\alpha \rightarrow 0$ with $\alpha\beta = \chi > 0$ fixed, the solution w of (11) converges along subsequences to a solution of*

$$-\Delta w + \chi((\theta_h^R + w)^4 - \theta_f^4) = 0, \tag{17}$$

with $w \rightarrow 0$ as $r \rightarrow \infty$.

Proof. In view of the *a priori* bounds on w and on R , and in view of Remark 4 we know that w , w' and w'' are (uniformly) equicontinuous on bounded balls. This suffices again to conclude that, as $\alpha \rightarrow 0$, a subsequence converges in $C^2(\overline{B_\rho})$, for any $\rho > 0$, to a solution of (17). As before, a diagonal process finishes the proof. □

Remark 11. *In this limit w remains non-trivial in the sense that it does not coincide with one of the bounds in (12). Thus, in the limit we will have a bifurcation diagram given by*

$$\frac{Y_f}{\text{Le}R} = F\left(\theta_f + \frac{Y_f}{\text{Le}} + w(R)\right),$$

and the right hand side truly depends on R .

4 Numerical calculations

In this section we examine the flame balls numerically. We will compare the outcome of the computations with analytic formulas for the “linearized” problem, which we present below.

4.1 Analytic solutions for the linear case

In this first part, we derive a bifurcation diagram equation for the linear case. Namely, we still consider Problem (4), except that (4c) is replaced by the linear equation

$$-\Delta u + 3\alpha^2 u - \alpha \Delta \theta = 0. \quad (18)$$

We can compute explicit formulas for the temperature θ and the variable u . To simplify the notation we introduce

$$\mu = \mu_{\alpha\beta} = \sqrt{3\alpha^2 + \alpha\beta}.$$

Then

$$\theta(r) = \begin{cases} \frac{B_1}{r} \sinh(\mu r) + B_3 + \theta_f & \text{for } r \leq R, \\ \frac{B_2}{r} \exp(-\mu r) + \frac{B_3 R}{r} + \theta_f & \text{for } r > R, \end{cases}$$

where the constants are given by

$$B_1 = \frac{\alpha\beta Y_f}{\text{Le}\mu^3} \exp(-\mu R), \quad B_2 = \frac{\alpha\beta Y_f}{\text{Le}\mu^3} \sinh(\mu R), \quad B_3 = \frac{3\alpha^2 Y_f}{\text{Le}\mu^2}.$$

The expression for u is

$$u(r) = \begin{cases} -\frac{B_1 \mu^2}{\beta r} \sinh(\mu r) & \text{for } r \leq R, \\ -\frac{B_2 \mu^2}{\beta r} \exp(-\mu r) & \text{for } r > R. \end{cases}$$

Finally, the equation that fixes the flame radius R , and that determines the bifurcation diagrams, reads

$$F\left(\frac{\alpha\beta Y_f}{2\mu^3 \text{Le} R} [1 - 2\mu R - e^{-2\mu R}] + \frac{Y_f}{\text{Le}} + \theta_f\right) = \frac{Y_f}{\text{Le} R}. \quad (19)$$

4.2 Bifurcation diagrams

Let us turn to the numerical investigation of the problem. Since we know from Theorem 1 that a solution is uniquely determined by its flame radius R , we exhibit diagrams in which the flame ball is represented by R along the vertical axis, and the horizontal axis is reserved for a control parameter, such as Y_f or one of the radiative parameters α or β .

We can only do numerical simulations on bounded domains, so we choose a large ball B_ρ on which we impose Dirichlet boundary conditions, as used in the existence proof. From the proof of Lemma 4 we know that the solution on the bounded ball B_ρ approaches the solution on \mathbb{R}^3 as $\rho \rightarrow \infty$, and in the numerical calculations we always make sure that $\rho \gg R$. Since

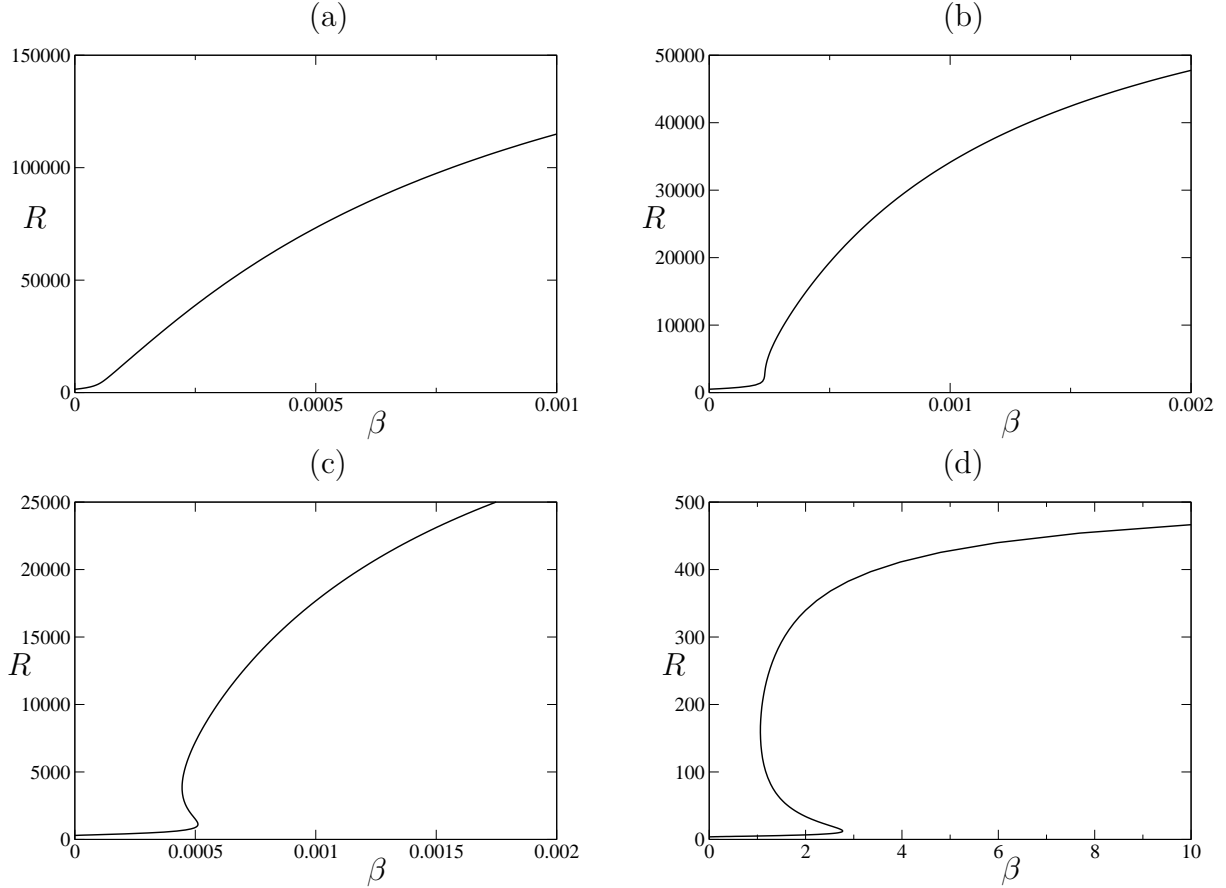


Figure 5: Bifurcation diagrams with β as the bifurcation parameter for (a) $A = 0.1$; (b) $A = 0.3$; (c) $A = 0.5$; (d) $A = 40$.

the flame balls are radially symmetric, the problem is thus reduced to a boundary value problem for an ODE, and we use the continuation software [21] to compute the bifurcation diagrams.

We need an explicit expression for the reaction rate. Following the literature, e.g. [22, 23], we choose a simple Arrhenius law

$$F(\theta(R)) = A \exp\left(-\frac{1}{\varepsilon\theta(R)}\right), \quad (20)$$

where ε is a normalized inverse activation energy and $A > 0$ is the pre-exponential factor. Next we must choose values for the parameters. Unless mentioned otherwise, in all computations we take

$$\theta_f = 1, \quad Y_f = 1, \quad \text{Le} = 1, \quad \varepsilon = 0.1, \quad A = 40, \quad \alpha = 10^{-4}, \quad \beta = 2.$$

In fact, the parameters Y_f and Le appear in the stationary problem only in the combination Y_f/Le , so we will use this ratio as a parameter in what follows.

In Figure 5 bifurcation diagrams are shown with β as the bifurcation parameter, for various values of the pre-exponential constant A . We see that a turning point appears in the bifurcation diagram as we increase A . Hence, for A sufficiently large there is a range of values

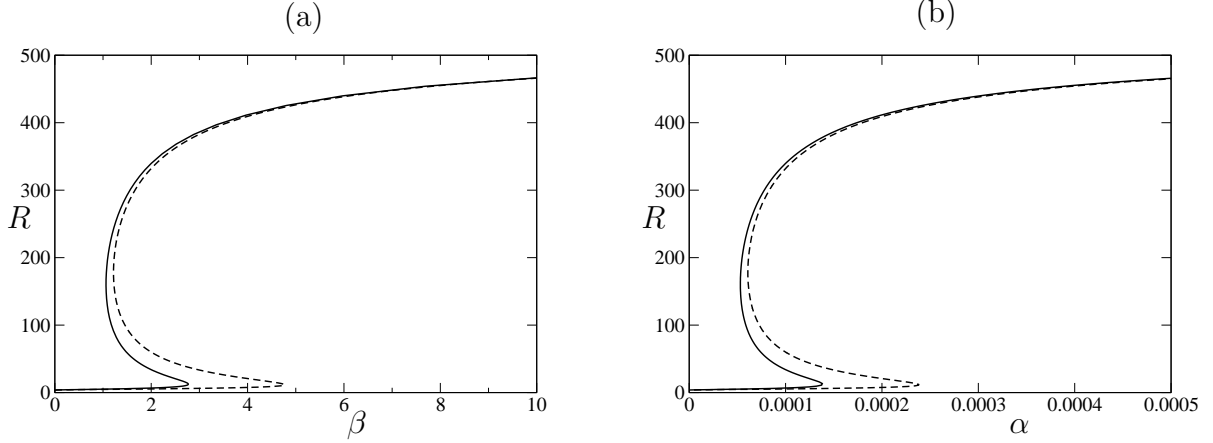


Figure 6: Comparison between the nonlinear problem (solid line) and the linearized one (dashed line) with (a) β and (b) α as the bifurcation parameter.

of the Boltzmann number β for which there exist multiple stationary flame balls. Increasing A corresponds to making the function in the Arrhenius law (20) steeper. In the context of traveling wave solutions (moving flame fronts) it was already observed (and extensively analyzed) that a steeper Arrhenius law may lead to turning points in bifurcation diagrams, see [19]. We note that the presence of turning points is due to the radiative effects being incorporated in the model, since uniqueness of the adiabatic flame ball implies the absence of turning points in the adiabatic problem.

Figure 5 also corroborates the study of the limit cases in Section 3. In the limit $\beta \rightarrow 0$ the flame radius R converges to the Zeldovich radius (the minimal possible radius), see Remarks 2 and 10. On the other hand, as proved in Lemma 11, in the limit $\beta \rightarrow \infty$ the temperature profile converges to θ_f , which corresponds to the maximal radius (see again Remark 2).

To make a useful comparison between the full, nonlinear problem and the “linearized” equation (18) from Section 4.1, we need to linearize the term θ^4 around some *characteristic temperature* θ_c : $\theta^4 \approx \theta_c^4 + 4\theta_c^3(\theta - \theta_c)$. Introducing the rescaled variable $\tilde{u} = \beta u$, we then arrive at the system

$$\begin{cases} \Delta\theta + \tilde{u} = 0, \\ \Delta\tilde{u} - 3\alpha^2\tilde{u} + 4\alpha\beta\theta_c^3\Delta\theta = 0. \end{cases}$$

Therefore, solutions of the full problem should be compared to solutions of the linearized problem for $\tilde{\beta} = 4\beta\theta_c^3$. Hence, in all figures, for the (dashed) curves representing the analytic expression (19) for the linearized problem, the scaling factor $4\theta_c^3$ is taken into account. As characteristic temperature we simply adopt $\theta_c = \theta_f$ throughout.

In Figure 6 we compare the outcome of the numerical computations on the nonlinear problem with the analytic expression for the linearized one, using both α and β as bifurcation parameters. In Figure 6a we see that the nonlinear and linear problems are qualitatively very similar. In the limit $\beta \rightarrow \infty$ we know from Lemma 11 that $\theta \rightarrow \theta_f$ uniformly, so our choice of $\theta_c = \theta_f$ leads to quantitative agreement for large β . In the adiabatic limit, i.e. $\beta \rightarrow 0$, the solution becomes independent of the radiative effect, irrespective of the equations being

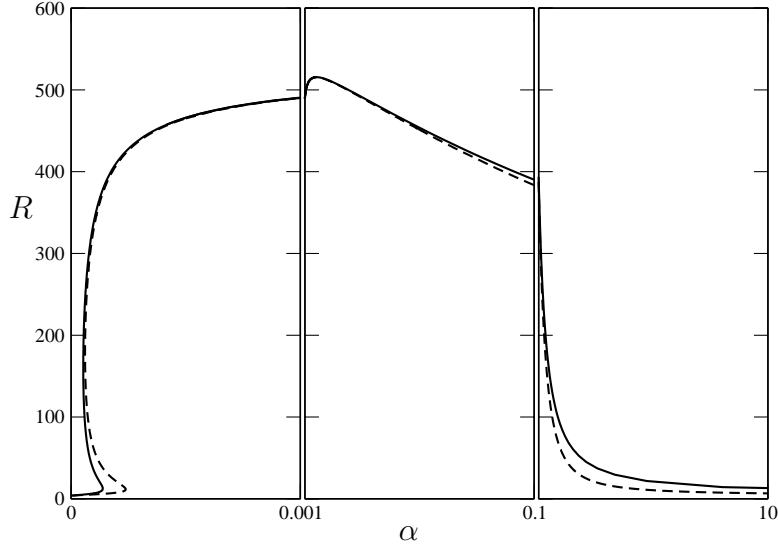


Figure 7: The complete (α, R) bifurcation diagram, on three different scales.

linear or not.

Figure 6b is, up to a scaling in the horizontal direction, the same as Figure 6a. The reason is that α is so small that α^2 is negligible compared to $\alpha\beta$, so that to good approximation the solution in this parameter regime only depends on the combination $\alpha\beta$.

From Lemma 9 we know that for large α the solution converges to the adiabatic one, and the radius decreases towards the Zeldovich radius. Indeed, when we continue the bifurcation curve of Figure 6b for larger values of α we obtain Figure 7, where we need three different scales to be able to see the full picture. In accordance with Lemmas 9 and 10 the flame radius R tends to the $\frac{Y_f}{Le} \frac{1}{F(\theta_f + Y_f/Le)}$ in both limits $\alpha \rightarrow 0$ and $\alpha \rightarrow \infty$, while it makes an excursion near $\frac{Y_f}{Le} \frac{1}{F(\theta_f)}$ in between.

In Figure 8 we employ Y_f/Le as the bifurcation parameter. For Y_f/Le sufficiently large there are again three solutions, and we need to examine two different scales to see them. The linearized problem does not mimic the nonlinear one too closely, since for large values of Y_f/Le the temperature varies too much to be adequately represented by the characteristic temperature θ_c .

The linear behavior of the curves in Figure 8 can be understood from the fact that α is chosen very small. In this asymptotic regime it is not hard to calculate the slopes for the linearized problem. In fact $R \sim C_i \frac{Y_f}{Le}$, where the two slopes $C_{1,2}$ in Figure 8a are approximately given by the two largest solutions of $F(\frac{1}{2\sqrt{\alpha\beta}}C^{-1} + \theta_f) = C^{-1}$, while the slope C_3 in Figure 8b is approximately equal to A^{-1} . Of course, the reason we can determine these slopes is that we have the explicit expression (19) for the bifurcation curve in the linearized problem. For the nonlinear problem, determining the slopes is an exercise in asymptotic analysis that falls outside the scope of this paper. Note that near the origin the slope is given by $F(\theta_f)^{-1}$ for both the linearized and the nonlinear problem.

Finally, while Figure 8a suggests that there are two disconnected solution branches,

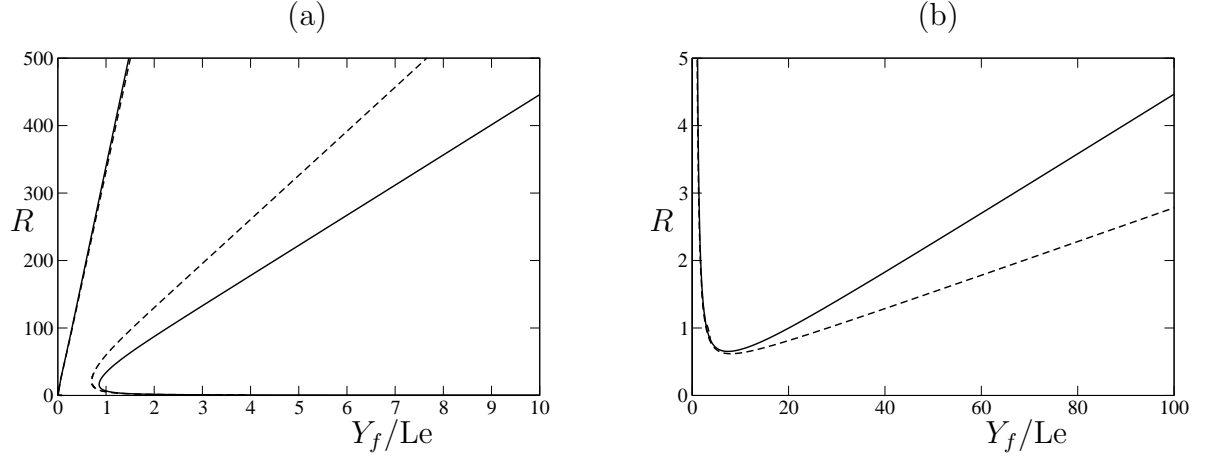


Figure 8: Comparison between the nonlinear problem (solid line) and the linearized one (dashed line) with Y_f/Le as bifurcation parameter, depicted at two different scales.

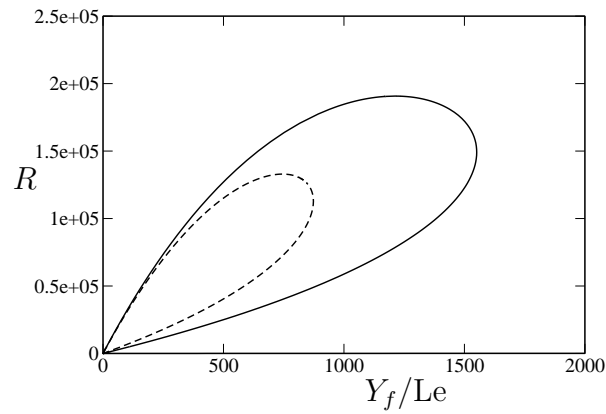


Figure 9: The global picture of the $(Y_f/Le, R)$ bifurcation diagram. Note that there is a branch of solutions (almost) coinciding with the horizontal axis.

the global bifurcation diagram depicted in Figure 9 shows that these branches are in fact connected to each other for large values of R and Y_f/Le .

The multiplicity of flame ball solutions, also found in heat loss models [7, 11], leads to questions about stability, which we intend to study in future work. As in the heat loss case, it is in these stability issues that the Lewis number, which plays a somewhat subdued role in the analysis of the stationary problem, will be crucial.

5 Conclusion

Radiation can significantly influence combustion processes. In this paper we investigate a free boundary model for combustion in a gaseous mixture, where we couple the usual diffusion equations to the radiation field. The radiation itself is described by the Eddington equation, which models radiative transfer in a dusty medium under (near) isotropic conditions. This model thus incorporates both emission and absorption of radiation, in contrast to the usual simplified heat loss models, cf. [4, 11]. Mathematically, this leads to the addition of an elliptic equation describing the radiation field, which is coupled to the (parabolic) diffusion equations.

In this context we prove the existence of radially symmetric stationary solutions, or *flame balls*, which are physically observed in micro-gravity environments [2]. We find that a solution exists for any combination of the parameters in the model. Since we consider a free boundary model, determining the radius of the flame is part of the problem. Our strategy is to split the analysis in two parts. First we fix the free boundary and solve an elliptic problem on a fixed domain. Subsequently, we solve the remaining algebraic equation to select the correct flame radius.

Having proved the existence of stationary flame balls, we then turn our attention to asymptotic regimes of the radiative parameters, namely the opacity α of the medium and the Boltzmann number β . In both the limits $\alpha \rightarrow 0$ and $\alpha \rightarrow \infty$ we recover the adiabatic (non-radiative, or “Zeldovich”) flames. The same limit is obtained in the limit $\beta \rightarrow 0$, whereas when $\beta \rightarrow \infty$ the temperature profile becomes flat. The limit $\alpha \rightarrow 0$, $\beta \rightarrow \infty$ with fixed $\alpha\beta$, leads to a nontrivial limit problem with a truly radiative asymptotic profile.

Finally, by using numerical computations and by examining analytically a “linearized” problem, we investigate the multiplicity of solutions (for fixed parameter values). We find large parameter regimes where multiple stationary flame balls exist. This of course raises interesting stability questions, which we plan to address in a forthcoming paper (extending the work of Joulin et al. [7] on the heat loss case). We expect the Lewis number Le , which is of minor importance for the stationary problem, to play a crucial role in the stability issues for radiative flame balls.

References

- [1] Y.B. Zeldovich, G.I. Barenblatt, V.B. Librovich, and G.M. Makhviladze. The mathematical theory of combustion and explosions. 1985.

- [2] P.D. Ronney, M.S. Wu, H.G. Pearlman, and K.J. Weiland. Experimental study of flame balls in space: Preliminary results from sts-83. *AIAA Journal*, 36:1361–1368, 1998.
- [3] http://exploration.grc.nasa.gov/combustion/sofball/sofball_index.htm.
- [4] G. Joulin and B. Deshaies. On radiation-affected flame propagation in gaseous mixtures seeded with inert particules. *Combust. Sci. and Tech.*, 47:299–315, 1986.
- [5] G. Joulin and M. Eudier. Radiation-dominated propagation and extinction of slow, particle-laden gaseous flames. *22nd Int. Symp. on combustion*, 1:1579–1585, 1988.
- [6] J.D. Buckmaster and T.L Jackson. The effects of radiation on the thermal-diffusive stability boundaries of premixed flames. *Comb. Sci. and Tech.*, 103:299–313, 1994.
- [7] J.D. Buckmaster and G. Joulin. The structure and stability of nonadiabatic flame balls. *Combustion and Flame*, 79:381–392, 1990.
- [8] C. Lederman, J.-M. Roquejoffre, and N. Wolansky. Mathematical justification of a nonlinear integrodifferential equation for the propagation of spherical flames. *Ann. Mat. Pura Appl.*, 183:173–239, 2004.
- [9] G.I. Sivashinsky. On flame propagation under condition of stoichiometry. *Siam J. Appl. Math.*, 39:67–82, 1980.
- [10] C.M. Brauner and A. Lunardi. Instabilities in a two-dimensional combustion model with free boundary. *Arch. Rational Mech. Anal.*, 154:157–182, 2000.
- [11] A.A. Shah, R.W. Thachter, and J.W. Dold. Stability of a spherical flame ball in a porous medium. *Combust. Theory Modelling*, 4:511–534, 2000.
- [12] D. Mihalas and B. Mihalas. *Foundation of radiation hydrodynamics*. Oxford University Press, 1984.
- [13] G.-C. Pomraning. *The equation of radiation hydrodynamics*. Pergamon Press, 1973.
- [14] B. Dubroca and J.L. Feugeas. Etude théorique et numérique d’une hiérarchie de modèles aux moments pour le transfert radiatif. *C. R. Acad. Sci. Paris I*, 329:915–920, 1999.
- [15] M.-N. Ozisik. *Radiative transfer*. Wiley, 1973.
- [16] M.-F. Modest. *Radiative heat transfer*. Series in Mechanical Engineering. McGraw-hill, Inc, 1993.
- [17] R. Siegel and J.R. Howell. *Thermal radiation heat transfer*. McGraw-Hill, Inc, 1972.
- [18] C.M. Brauner, J. Hulshof, and J.-F. Ripoll. Existence of travelling wave solutions in a combustion-radiation model. *Discrete and Continuous Dynamical Systems*, 1:193–208, 2001.

- [19] O. Baconneau, J.B. van den Berg, C.M. Brauner, and J. Hulshof. Multiplicity and stability of travelling wave solutions in a free boundary combustion-radiation problem. *European J. Appl. Math.*, 15:79–102, 2004.
- [20] L.C. Evans. *Partial Differential Equations*, volume 19 of *Graduate Studies in Mathematics*. American Mathematical Society, 1998.
- [21] E.J. Doedel, A.R. Champneys, T.F. Fairgrieve, Y.A. Kuznetsov, B. Sandstede, and X. Wang. Auto97, continuation and bifurcation software for ordinary differential equations (with homcont). 1997. Available by anonymous ftp from ftp.cs.concordia.ca, directory pub/doedel/auto.
- [22] F.A. Williams. *Combustion theory*. Addison Wesley, 1994.
- [23] J.D Buckmaster and G.S.S. Ludford. *Theory of laminar flames*. Cambridge University Press, 1982.